From vineyards to reshapable materials: α-CF 2 activation in 100% resveratrol-based catalyst-free vitrimers

Florian Cuminet, Sébastien Lemouzy, Éric Dantras, Éric Leclerc, Vincent Ladmiral, Sylvain Caillol

From vineyards to reshapable materials: α-CF_2 activation in 100 % resveratrol-based catalyst-free vitrimers

Received 00th January 20xx,
Accepted 00th January 20xx

DOI: 10.1039/x0xx00000x

Florian Cuminet,*[a,b] Sébastien Lemouzy,[a] Éric Dantras,[b] Éric Leclerc,[a] Vincent Ladmiral[a] and Sylvain Caillol*[a]

Vitrimers are a class of polymers bridging the gap between resistant crosslinked thermosets and recyclable linear thermoplastics. The first vitrimer ever described was a polyester network requiring relatively high catalyst loadings to be reshaped. This feature raises concerns about catalyst potentially leaching out of the materials and accelerated ageing upon reprocessing cycles. Recently, strategies such as activation of the exchange reaction by inductive effects or neighboring group participation have been implemented in vitrimers allowing to produce reshapable materials which do not require a catalyst. Hence, α,α-difluoro esters proved to be very prone to transesterification owing from the strong electron-withdrawing character of the CF_2 group resulting from the very high electronegativity of the fluorine atom. This feature implemented in polyester vitrimers enabled the synthesis of catalyst-free reshapable highly crosslinked networks. Moreover, this principle initially designed on petro-based monomers is here successfully adapted to resveratrol, a biobased polyphenol found in high concentration in grapes and Japanese knotweed (*Reynoutria japonica*). The material presented contains 86 % bio-based carbon, is catalyst-free, durable and recyclable and features a high T_g.

Introduction

[a] *ICGM, Univ Montpellier, CNRS, ENSCM, Montpellier, France.*
[b] *CIRIMAT, Université Toulouse 3 Paul Sabatier, Physique des Polymères, 118 Route de Narbonne, 31062 Toulouse, France.*

Electronic Supplementary Information (ESI) available: [1H, 13C, 19F NMR spectra, TGA, DSC, DMA thermograms, EEW calculation details, and fitting parameters for stress relaxation experiments]. See DOI: 10.1039/x0xx00000x

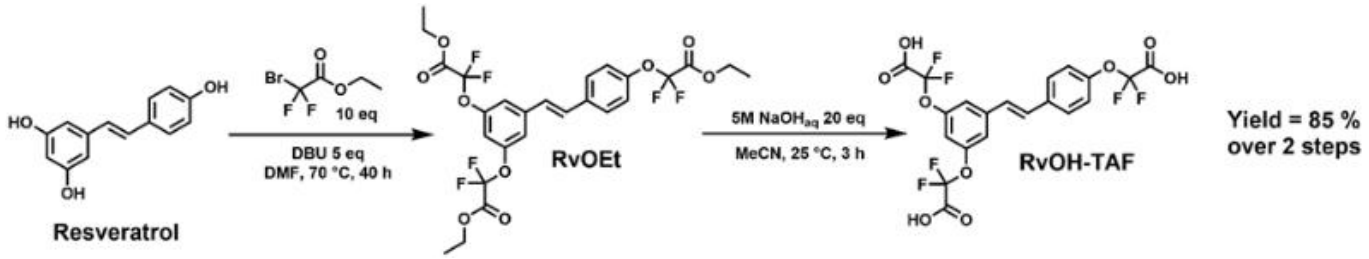

Scheme 1. 2-step synthesis of RvOH-TAF from resveratrol

Vitrimers are a class of polymer materials which exhibits excellent mechanical properties and the ability to be recycled mechanically.[1,2] Ideally, they combine the best of thermoplastics, which are often easily recyclable, and thermosets, which are endowed with very good mechanical properties and resistance at high temperature. These exceptional properties come from their structure. While thermoplastics are essentially a network of entangled linear chains which cohesion is due to weak bonds, thermosets are a tridimensional network made of strong covalent bonds.[3] Vitrimers are also 3D networks made of covalent bonds, but some of these bonds feature a singular property they are exchangeable with each other, or with free reactive groups on the polymer segments, by a degenerate chemical equilibrium.[4–7] These exchanges are usually activated by heat and are accountable for the vitrimers flow and recyclability at high temperature. Vitrimers were invented a decade ago, and first illustrated with polyesters able to flow thanks to a transesterification reaction.[8] They are of particular interest in the field of composites, in which the polymer matrix needs high mechanical performances and thermal resistance[9,10] but is very a challenge to recycle.[11,12] Vitrimers which can be reshaped upon heating and be depolymerized by solvolysis, could be a solution to address the issue of composites recycling.[13–15] However, for such applications it is desirable to obtain rigid materials with high T_g.[16–19] Fourteen examples of vitrimers with T_g above 100 °C were already reported. For instance, epoxy-anhydride vitrimers catalyzed by zinc (II) with T_g values up to 140 °C were described, but they required hard reprocessing conditions, at 250 °C under 500 bars.[20] A epoxy-acid system catalyzed by Sn(II) with 2 equivalents of epoxy compared to the acid allowed to reach a T_g at 231 °C thanks to the homopolymerization of the epoxy.[21] However, the resulting ether bonds cannot be reversibly cleaved in the reshaping conditions, which therefore limits the material reprocessability. Furthermore, in the case of transesterification vitrimers, an external catalyst is usually required to accelerate the transesterification reaction, so that the material may flow at a measurable timescale and be recycled.[22] The use of catalysts such as zinc(II) and triazabicyclodecene (TBD) raises concerns about potential leaching of the catalyst out of the material, and premature ageing of the vitrimer after several recycling/reshaping cycles.[23–25] For these reasons, the use of catalyst-free vitrimers is preferable. A first strategy is to use other exchange reactions, for instance vinylogous urethanes,[26] polythiourethanes,[27] disulfides,[28,29] imine bonds,[30–33] silyl ethers,[34] and Si-O-Ph bonds.[35] Several other strategies were described to make catalyst-free vitrimers, in particular in the case of transesterification vitrimers. Hyperbranched vitrimers featuring a loose network allowed catalyst-free reprocessing, but their mechanical properties were fairly limited.[36] A high concentration of free hydroxyl groups in the network also accelerates the transesterification, but it implies limitations in terms of accessible monomers and network structures and properties, and may increase the water intake of such materials.[37,38] The kinetics of the exchange reaction can also be increased by an activating group, linked to the network, in proximity to the exchangeable bonds.[39,40] In particular, fluorinated esters were recently proven to undergo fast transesterification without the recourse to an external catalyst, both in solution[41] and in vitrimers.[42,43] Furthermore, in a context of increasing tension on crude oil supply and price volatility, the pursuit of biobased materials is of booming interest to increase polymers sustainability.[44–46] The first vitrimer was partly biobased as the polyfunctional carboxylic acid used was made from dimers and trimers of fatty acids.[8] Many naturally occurring building blocks can be used in the synthesis of vitrimers, such as lignins, phenols, furans, oils, polysaccharides, carboxylic acids or natural rubber.[47] In particular, several examples of biobased vitrimers based on natural phenols such as vanillin,[48–50] eugenol[51,52] or cardanol[53] for instance have been reported. However, only few of them exhibit a T_g over 100 °C and high thermal stability, two precious properties for biobased vitrimers.[54] Some example of catalyzed biobased vitrimers with high T_g were described[55,56] but only two examples of high-T_g catalyst-free biobased vitrimers were reported. The first example is based on acetal exchange, with a T_g up to 121 °C.[57] The other example is based on transesterification activated by tertiary amines in polybenzoxazines, with T_g ranging from 143 to 193 °C.[58] Many of the high-T_g vitrimers reported so far are based on monomers featuring aromatic structures. Biobased phenols and furans,[47] thanks to their aromatic cycles and often compact structures, can provide high crosslinking density, rigidity, high T_g and thermal resistance to vitrimers.

In the work presented here, a catalyst-free, high T_g biobased

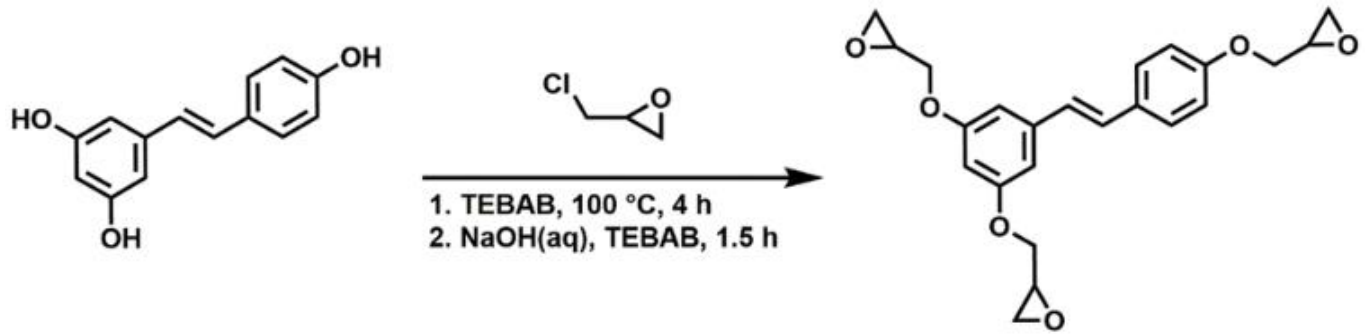

Scheme 2. Synthesis of epoxydized resveratrol RvOGly

transesterification vitrimer was synthesized from resveratrol, a biobased triphenol mainly found in grapes, peanuts and a plant called *Japanese knotweed (Reynoutria japonica)*.[59,60] Resveratol can be obtained from the rhizomes of this invasive plant for its valorization after uprooting.[61,62] The goal was to achieve high mechanical properties and reach high T_g thanks to the high aromatic carbon content of this bioresource. Resveratrol was functionalized to prepare two building blocks: a trifunctional epoxy, and a trifunctional α,α-difluorocarboxylic acid. The rationale was that the ring-opening polyaddition of these building blocks would lead to a dense network, endowed with high T_g and transesterification capability via fluorine group activation.

Results and Discussion

α,α-Difluoro Carboxylic Acid Monomer Synthesis

α,α-Difluoro carboxylic acids were proven to activate the transesterification reaction in polyester networks, without the need for any catalyst, thus enabling the synthesis of catalyst-free transesterification vitrimers.[41,43] A biobased tris α,α-difluoro carboxylic acid was synthesized from resveratrol (a biobased compound extracted from grapes). Starting from the triphenol, a 2-step synthesis led to the desired monomer. Resveratrol could be easily functionalized via Williamson-type etherification in the presence of ethyl bromodifluoroacetate at 70 °C for 40 hours.[63,64] Dimethylformamide (DMF) was used for the feasibility study, but a 1:1 mix of green solvents γ-valerolactone and dihydrolevoglucosenone (Cyrene™) could also be used as a greener alternative. After a filtration on silica gel, the expected α,α-difluoro triester (RvOEt) was obtained in 87 % yield. The isolated tris (ethyl ester) product underwent facile saponification in mild conditions to yield, after appropriate workup, the desired α,α-difluoro triacid (RvOH-TAF) as a brown waxy solid with an overall yield of 85 % and a biobased carbon content of 70 % (Scheme 1).

Trifunctional Epoxy Synthesis

In parallel to the modification of resveratrol into an activated trifunctional acid, this triphenol was also functionalized with epichlorohydrin to yield a trifunctional epoxy (Scheme 2). The glycidylation of phenols is very efficient, easily scalable and was extensively described already on biobased phenols including resveratrol.[65–68] The targeted building block RvOGly was prepared in large quantities (> 40g) by simple reaction of resveratrol with epichlorohydrin and tetrabutylammonium bromide (TEBAB). RvOGly features high functionality (EEW = 185 g/eq) and a 52 % aromatic carbon content (for RvOGly alone), close to the 57 % value of bisphenol A diglycidyl ether (BADGE), two features which are beneficial to obtain materials with high T_g.

Polymerization and Curing

RvOGly and RvOH-TAF were mixed at room temperature (ca. 20 °C) in PTFE molds to avoid any transfer step, because of the fast gelation of the mixture even at room temperature (ca. 20 °C). The reaction between both monomers was exothermic and the mixing step needed to be performed on small scale, typically 1-2 g, to better control the heat transfer and to avoid gelation before complete mixing. This fast gelation is caused by the strong activation of the carboxylic acids toward the epoxy opening by the fluorine atoms. A reaction on larger scales may benefit from the addition of a solvent to control the heat release. This pathway was not explored in this study though, to avoid the plasticizing effect of potential residual solvent and its effect on mechanical properties. The mixture formed a material within a few minutes, and was left at room temperature for 3 h.

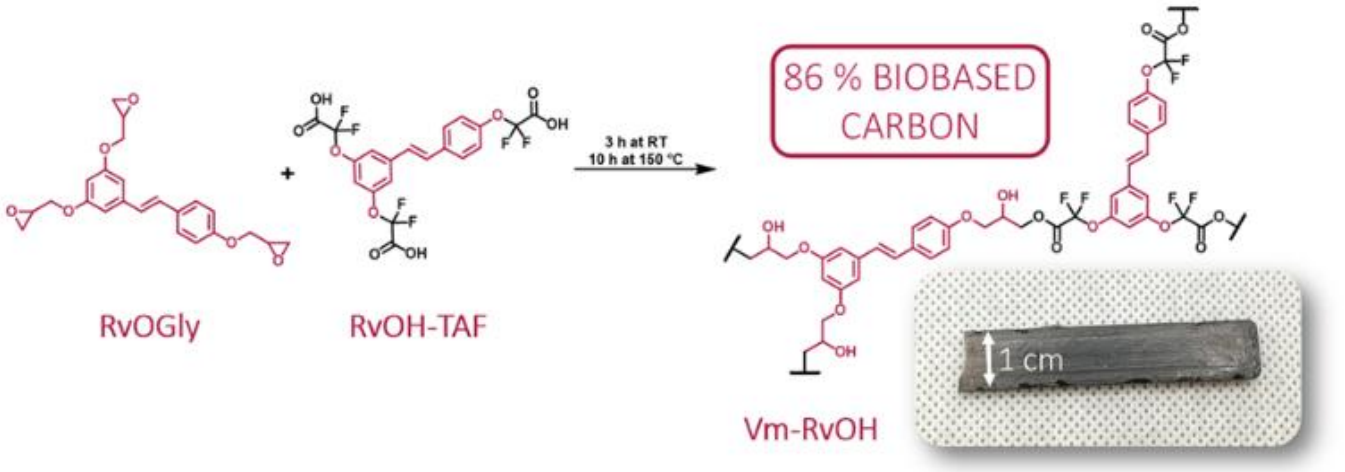

Figure 1. Polymerization of RvOGly and RvOH-TAF resulting into the Vm-RvOH material, insert : optical image of Vm-RvOH (1 cm x 4.5 cm x 0.3 cm)

The curing was checked by DSC (Figure S9). On the first heating ramp, an exothermic enthalpy is visible starting from 150 °C. On the second ramp this phenomenon does not appear and a T_g is visible in the 100-130 °C range. The exothermic phenomenon was attributed to a residual polymerization occuring when the material is heated higher than 150 °C. Thus, a 1 h curing step at 150 °C was applied and the DSC analysis was repeated (Figure S10). After this curing step, two consecutive heating ramps overlaid almost perfectly. There

was no sign of ongoing polymerization by DSC. The curing was also checked by mechanical analysis. The evolution of the modulus was monitored with time at 150 °C. The stabilization of the value happened after 7 h (Figure S11). Therefore, the materials were left 10 h at 150 °C to ensure complete polymerization, resulting in a hard brittle dark brown material (Vm-RvOH, Figure 1). The resulting material exhibits a 86 % biobased carbon content.

Vitrimer Characterization

After complete polymerization three consecutive DSC ramps were carried out on the resulting material. The first ramp was meant to erase the thermal history of the material, then the thermograms of the second and third ramps overlaid perfectly, and no residual exotherm was observed. The T_g is visible in the 92-125 °C range, but the transition is broad and the ΔCp is low (0.241 $J.g^{-1}.K^{-1}$). Therefore, the T_g was determined as the minimum of the heat flow derivative, at 117 °C (Figure S12 and Table 1). The high T_g compared to previously reported covalent adaptable networks[42,43] was expected because of the high aromatic carbon content of the polymer (56 % aromatic carbon content for the polymer). This value of T_g is comparable to that of the catalyst-free biobased vitrimer synthesized from lignin by Moreno et al.[57] (T_g = 121 °C), but lower than the value of the catalyst-free biobased polybenzoxazine vitrimers recently reported by Adjaoud et al. (T_g from 143 to 193 °C).[17] This last case benefits from a 50 % aromatic carbon content, close to the 56 % value reported here, but also a 17 % cycloaliphatic carbon content caused by the isosorbide core of its monomer, which brings additional rigidity. Thus, the performance of Vm-RvOH in term of T_g is consistent with its structure.

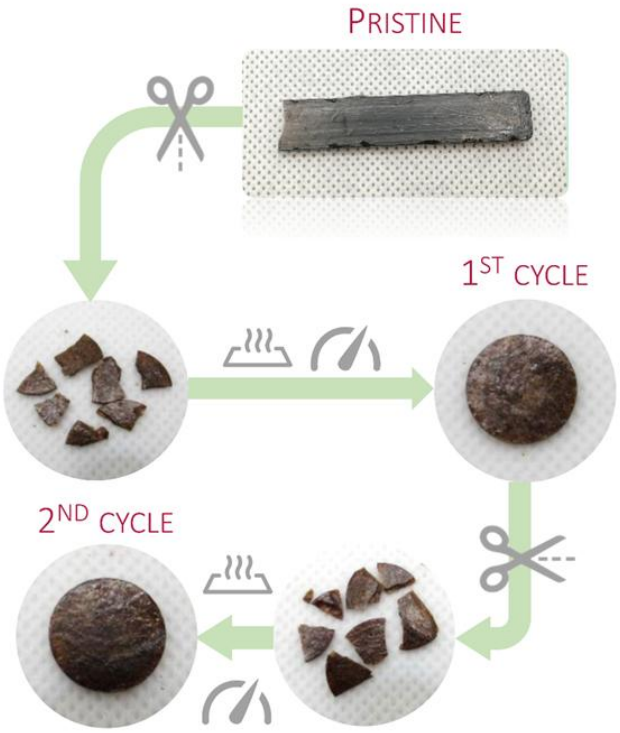

Figure 2. Vm-RvOH reprocessing for 2 h at 170 °C under 80 bars (scale of pristine material: 1 cm x 4.5 cm x 0.3 cm, diameter of recycled materials: 1 cm)

A DMA analysis was also performed to confirm the results observed by DSC, and to characterize the mechanical properties of the material (Figure S13). T_α was determined as the maximum of the loss modulus E" at 94 °C. As observed by DSC, the mechanical relaxation was broad and the temperature of the maximum of tan(δ) was 117 °C, which is consistent with the T_g measured by DSC. The moduli on the glassy plateau and on the rubbery plateau were respectively E'_G = 2.1 GPa and E'_R = 46 MPa. The modulus on the glassy plateau is comparable to values reported for a material made from epoxydized resveratrol and 4,4'-diaminodicyclohexylmethane (PACM),[68] and with the value of a lignin-based catalyst-free vitrimer.[57] For the modulus on the rubbery plateau, the value for Vm-RvOH is 14 times lower than the epoxydized resveratrol-PACM thermoset,[68] but still in the 11-73 MPa range reported for other high-T_g vitrimers,[18,21] included for aerospace applications.[29] Additionally, this value is 2.5 times higher than the value reported on the similar α,α-difluoro vitrimer previously reported.[43] At temperatures over 200 °C, the modulus decreases from the rubbery plateau. This could be the manifestation of the beginning of the flow.

The thermal stability of Vm-RvOH was assessed by TGA under nitrogen. The 2 % and 5 % degradation temperatures $T_{d2\%}$ and $T_{d5\%}$ were 237 °C and 275 °C respectively (Figure S14 and Table 1). The residue at 900 °C under nitrogen was 28.9 % of the initial weight. The $T_{d5\%}$ value is low compared to the values superior to 300 °C reported for other high-T_g vitrimers,[18,32,33,35,56,69] but still higher than the value at 224 °C for a lignin-based catalyst-free vitrimer.[57] The residue (char yield) was comparable with an epoxy vitrimer in the same range of T_g.[31] The relatively high char yield depends essentially on the monomers structures, thanks to the high aromatic carbon content (56 %).

Solubility tests were performed in THF (which easily solubilizes both resveratrol-based precursors). After stirring for 24 hours, a swelling of 278 % and an insoluble fraction of 73 ± 2 % were measured. This result seemed low for a 3+3 crosslinked

Table 1. Physicochemical main properties of Vm-RvOH

T_g (°C)	T_α (°C)[a]	Max tan(δ) (°C)	E'_G (GPa)[b]	E'_R (MPa)[c]	Gel content (%)[d]	Swelling index (%)[d]	$T_{d\,2\%}$ (°C)[e]	$T_{d\,5\%}$ (°C)[e]	Residue (char) (%)[f]	Weight loss (%)[g]
117	94	117	2.1	46	100±1	68	237	275	28.9	2.9

[a] determined as the maximum of E" | [b] at T_α – 50 °C | [c] at T_α + 50 °C | [d] in anhydrous THF | [e] N_2 atmosphere | [f] at 900 °C, N_2 atmosphere | [g] after 6 h at 170 °C, air atmosphere

material, and might be attributed to hydrolysis due to water in the THF. Therefore, it was repeated in anhydrous THF. A swelling of 68 % and a gel content of 100 ± 1 % was found (Table 1). These results prove the formation of a 3D crosslinked material.

Reprocessing trials were performed on Vm-RvOH by compression molding. In a previous study on a similar system, the reprocessing temperature was set at 100 °C, 50 °C above the T_g, under 16 bars.[43] At 170 °C, the material could be reprocessed in 2 h under 80 bars (Figure 2). The reprocessing temperature is 50 °C above the T_g, like the previous system. The pressure applied is lower than for many high-T_g vitrimers, which often require a pressure of at least 100 bars.[28,32,35,56,70]

The thermal stability of the material at this reprocessing temperature was assessed. An isothermal experiment at 170 °C was performed in air atmosphere, to simulate the reprocessing conditions (Figure S15). After 2 h, the relative mass loss was 2.48 %. Between 2 h and 4 h the additional mass loss was 0.29 % and between 4 h and 6 h, 0.47 % to attain an overall mass loss after 6 h around 3 %. This value is small, but cannot be ignored. Reprocessing trials were made at 170 °C under 80 bars. Therefore, the DMA analysis of the material needs to be assessed and compared before and after reprocessing at 170 °C, to monitor a possible degradation. Two consecutive reprocessing cycles at 170 °C were made, and the mechanical properties after each cycle were studied by DMA (Figure 3).

The value of the modulus on the glassy plateau remains quasi-constant. The value of T_α decreased from 94 to 75 °C after the first reprocessing cycle, and remained at 76 °C after the second cycle (Table 2). Similarly, the values of the modulus on the rubbery plateau E'_R decreased from 46 to 23 MPa with the first reprocessing, and then remained the same after the second cycle. These results suggest a decrease of the crosslinking density upon the first cycle, which might be due to a slight hydrolysis at the reprocessing temperature. Then the crosslinking density remains constant for the subsequent cycle, thus the hydrolysis remains very limited. This is likely due to the aromatic carbon content (56 % aromatic carbon) which brings a hydrophobic behavior to the material and balances the hydrophilic behavior brought by the esters and hydroxyl groups. Moreover, the high T_g probably plays an important role, as the water uptake is very limited when the material is in the glassy state, but much easier in the rubbery state. Indeed, in the rubbery state, the mobility of the polymer makes easier the penetration of water in the network. Finally, the results obtained by DMA were confirmed by DSC, with a T_g of 117 °C for the pristine material, 97 °C after the first reprocessing and 91 °C after the second cycle.

Table 2. Evolution of the thermomechanical properties of Vm-RvOH with reprocessing cycles.

Reprocessing Cycle	T_g (°C)	T_α (°C)[a]	Max tan(δ) (°C)	E'_G (GPa)[b]	E'_R (MPa)[c]
Pristine	117	94	117	2.1	46
Reprocessed once	97	75	101	2.4	23
Reprocessed twice	91	76	104	2.7	23

[a] determined as the maximum of E" | [b] at T_α – 50 °C | [c] at T_α + 50 °C

The flow from the rubbery plateau was studied by isothermal stress-relaxation experiments to evaluate the kinetics of this phenomenon (Figure S16). The modulus of the material was monitored under a 0.3 % strain between 170 and 210 °C. For all temperatures, a plateau around 5 % was reached at the end of the relaxation experiment. This is likely due to a proportion of permanent linkages in the network. The presence of such permanent linkages can be explained by a minor homopolymerization of the epoxy.[21] Indeed, the strong acidity of α,α-difluoro acids may favor this reaction.[21]

The stress-relaxation experiments were normalized, and a Kohlrausch-Williams-Watts "stretched exponential" equation with an added constant y_0 was used to fit the experimental data (Figure 4 and Table S1). The constant y_0 translates the

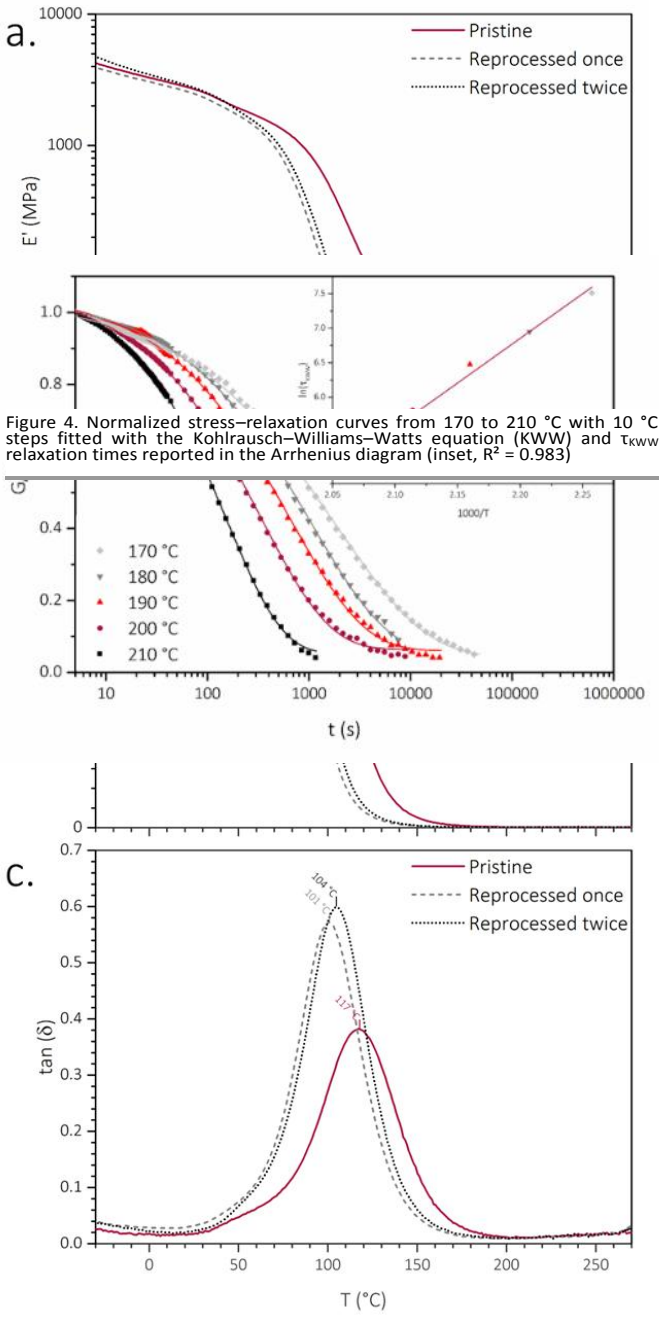

Figure 4. Normalized stress–relaxation curves from 170 to 210 °C with 10 °C steps fitted with the Kohlrausch–Williams–Watts equation (KWW) and τ_{KWW} relaxation times reported in the Arrhenius diagram (inset, $R^2 = 0.983$)

final plateau of the relaxation, and the stretch parameter β translates a distribution of behaviors centered on the value of the relaxation time τ_{KWW}. The closer to 1 β is, the narrower the distribution is. This parameter is linked to the heterogeneity in the vicinity of the exchangeable bond. Here, the values of β ranged between 0.486 at 170 °C and 0.797 at 210 °C and increased with the temperature. The broad distribution might be due to the influence of weak bonds hindering the relaxation. The number of weak bonds probably decreases when the temperature increases, which would result in an increasingly homogeneous behavior of the exchangeable bonds, and the increasing value of β. The constant added y_0 allowed a better accuracy on the fitting, with $0.99264 \leq R^2 \leq 0.99639$ without constant and R^2 = 0.99937 to 0.99979 with a constant. The mean value of this constant y_0 (Table S1) is 0.054 (values between 0.043 and 0.064). Thus, a mere 5 % of the applied stress is not relaxed because of the permanent linkages, which does not impede the reprocessing of the material.

The relaxation times τ_{KWW} obtained for each temperature were plotted in an Arrhenius diagram (Figure 4 inset). A linear fit was obtained (R^2 = 0.983) and the flow activation was calculated from the slope E_a = 107 kJ mol^{-1}, in accordance with the 29-163 kJ mol^{-1} range reported for transesterification vitrimers.[40] This E_a is higher than that reported in previous studies of transesterification vitrimers activated by fluorinated groups (67-77 kJ mol^{-1}).[42,43] It is likely caused by the higher crosslinking density and lower mobility at the local scale of Vm-RvOH.

Conclusions

A catalyst-free polyester vitrimer was synthesized from resveratrol, a biobased triphenol found mainly in grapes. This material exhibits a high biobased carbon content of 86 %. A trifunctional epoxy and a trifunctional α,α-difluoro carboxylic acid were synthesized by functionalization of resveratrol with epichlorohydrin and ethyl bromodifluoroacetate, respectively. When these two resveratrol derivatives were mixed together, the ring opening polymerization of the epoxy by the carboxylic acid occurred at room temperature owing from the increased acidity of the carboxylic acid O-H bond due to the neighboring electronegative fluorine atoms. After a curing step at 150 °C, a rigid slightly brittle material was obtained. This material exhibited a high T_g (117 °C), comparable to other high-T_g vitrimers,[28,31,71,72] which makes it relevant for structural applications. The synthesis described could be adapted to other biobased compounds with similar structures and higher functionality, such as quercetin, to reach even higher T_g values. Moreover, the α,α-difluoro esters can exchange with free hydroxyl groups without any added catalyst. This feature allows the efficient reprocessing of the material at 170 °C for 2 h by compression molding. Two recycling cycles were achieved and the mechanical performance remained worthwhile for structural applications. This material is one of the first high-T_g catalyst-free biobased vitrimers.[17,57]

Experimental section

Materials

Trans-Resveratrol (Fluorochem, 98 %), 1,8-Diazabicyclo(5.4.0)undec-7-ene (DBU, Fluorochem, 98 %), ethyl bromodifluoroacetate (Fluorochem, 98 %), epichlorohydrin (Sigma-Aldrich, ≥ 99 %), tetrabutylammonium bromide (TCI, > 98 %), benzophenone (Avocado Research Chemicals Ltd, 99 %), were used as received. Dimethylformamide (DMF, ≥ 99.5 %), tetrahydrofuran (THF, ≥ 99 %) and $NaHCO_3$ were supplied by VWR Chemicals, diethyl ether (≥ 99.5 %) and pentane (≥ 95 %) were supplied by Carlo Erba, ethyl acetate (≥ 99 %) was supplied by Fisher Chemicals, acetonitrile (≥ 99.9 %) was supplied by Acros Organics, sodium hydroxide (≥ 98 %) and chlorohydric acid ≥ 37 % were supplied by Honeywell Fluka, anhydrous THF was supplied by Carlo Erba (anhydrous for analysis stabilized with BHT, on 4A molecular sieve). Deuterated solvents were supplied by Eurisotop (99.8 %). γ-valerolactone (GVL, BioRenewable, ≥ 99 %) and dihydrolevoglucosenone (Cyrene™, BioRenewable, ≥ 98.5 %) were obtained from Sigma-Aldrich.

Synthetic Procedures

"RvOEt" compound:[63,64]* Trans-Resveratrol (3,5,4'-trihydroxy-trans-stilbene, 2.3 g, 10 mmol, 1 eq) was dissolved in dry DMF (60 mL, 0.16 M). 1,8-Diazabicyclo [5.4.0] undec-7-ene (DBU, 7.5 mL, 50 mmol, 5 eq) was added in one portion and the reaction was heated to 70 °C. Ethyl bromodifluoroacetate (6.4 mL, 50 mmol, 5 eq) was then added via a syringe pump at a rate of 5.0 $mL.h^{-1}$ and the reaction was stirred at 70 °C for 40 h. The crude mixture was cooled to room temperature, diluted with H_2O (300 mL), and extracted 5 times with Et_2O (5 x 50 mL). The combined organic layers were washed twice with water and once with brine, dried with Na_2SO_4, filtered, and concentrated under reduced pressure to obtain a dark red oil. The crude mixture was purified by filtration on silica gel using pentane/ethyl acetate (1:1) to afford the pure triester (6 g, 87 %, clear brown viscous liquid).

Triester RvOEt characterizations (NMR spectra in Figures S1 to S3: ^{1}H NMR 400MHz $CDCl_3$: δ 7.50 (m, 2H, aromatic protons), 7.25 – 7.21 (m, 4H, aromatic protons and C=C), 7.11 – 6.95 (m, 3H, aromatic protons), 4.40 (2q, ^3J = 8 Hz, 6H, $OC\underline{\mathbf{H_2}}CH_3$), 1.37 (2t, ^3J = 8 Hz, 9H, $OCH_2C\underline{\mathbf{H_3}}$). ^{19}F NMR 377 MHz, $CDCl_3$: δ -76.30, -76.53. ^{13}C NMR 101 MHz, $CDCl_3$: δ 159.9 (m, $\underline{\mathbf{C}}O_2Et$), 150.3 (m), 150.2 (m), 140.1, 134.7, 130.3, 128.1, 127.1, 122.0, 117.4, 114.1 (t, $^1J_{C-F}$ = 1021 Hz, OCF_2),), 114.0 (t, $^1J_{C-F}$ = 1025 Hz, OCF_2), 64.0 (O-$\underline{\mathbf{CH_2}}CH_3$), 63.9 (O-$\underline{\mathbf{CH_2}}CH_3$), 14.0 (O-$CH_2\underline{\mathbf{CH_3}}$), 14.0 (O-$CH_2\underline{\mathbf{CH_3}}$). HRMS (ESI+) Calc. for $[M+H]^+$ 595.1397, found 595.1394.

"RvOH-TAF" compound: In a 250 mL round bottom flask, 6 g of triester were dissolved in acetonitrile (90 mL). Then, a 5 M aqueous solution of NaOH (12.5 g in 62 mL) was added slowly at room temperature, and the mixture was stirred for 3 h. 200 mL of a saturated $NaHCO_3$ solution was added to the mixture and the aqueous layer was washed with 100 mL of diethyl ether. The organic layer was extracted with 50 mL of saturated $NaHCO_3$ solution, and the gathered aqueous layers were acidified to pH=1 using 2 M HCl. Finally, the acidified aqueous

layer was extracted with 3 x 100 mL of diethyl ether, and the solvent was removed under high vacuum to afford 5 g of the desired triacid as a brown waxy solid (yield 98 %, yield over the two steps η = 85 %, purity > 98 % estimated from ^{1}H NMR spectrum).

Trifunctional acid TPE-TAF characterizations (NMR spectra in Figures S4 to S6): ^{1}H NMR 400MHz d_6-DMSO: δ 7.72 (d, 2H), 7.59-7.13 (m, 5H, aromatic protons and C=C), 7.00 (s, 1H). ^{19}F NMR 377 MHz, d_6-DMSO: δ -76.16, -76.50. ^{13}C NMR 101 MHz, d_6-DMSO: δ 161.0 (COOH, t, $^{2}J_{C-F}$ = 39.0 Hz), 160.7 (COOH, t, $^{2}J_{C-F}$ = 39.0 Hz), 150.4 (ipso-ArC-O), 149.4, 140.8, 135.0, 130.6, 128.7, 127.1, 121.8, 117.3, 114.64 (OCF_2, t, $^{1}J_{C-F}$ = 272 Hz), 114.56 (OCF_2, t, $^{1}J_{C-F}$ = 274 Hz), 113.4. HRMS (ESI+) Calc. for $[M+H]^+$ 511.0458, found 511.0468. HRMS (ESI-) Calc. for $[M-H]^-$ 509.0313, found 509.0319.

"RvOGly" compound (glycidylation of resveratrol): In a 500 mL round bottom flask, 20.56 g (90 mmol, 1 eq) of resveratrol was dissolved in 82 mL (96 g, 1.04 mol, 12 eq) epichlorohydrin at room temperature under magnetic stirring. The flask was then equipped with a condenser and heated to 100 °C. 1.56 g (4.8 mmol, 0.05 eq) of tetrabutylammonium bromide "TEBAB" was added and the reaction was left to proceed under stirring at 100 °C for 4 h. Then, the reaction medium was cooled to room temperature and 20 wt% aqueous solution of NaOH and TEBAB was added (21 g NaOH + 1.56 g TEBAB in 106 mL deionized water). The mixture was left 1.5 h under vigorous stirring. The mixture was then diluted with 600 mL of water and extracted with 3 x 300 mL ethyl acetate. The organic layers were gathered, washed with 2 x 200 mL brine, dried on magnesium sulfate. The solvent was evaporated under reduced pressure to afford 42.3 g of a clear yellow viscous oil.

Epoxydized resveratrol RvOGly characterizations (NMR spectra in Figures S7 and S8): ^{1}H NMR 400MHz d_6-acetone: δ 7.52 (d, 2H), 7.29-6.99 (dd, 2H, C=C), 6.97 (m, 2H), 6.81 (d, 2H), 6.51 (t, 1H), 4.34 and 3.86 (3+3H), 3.33 (3H), 2.86 and 2.73 (3+3H). ^{13}C NMR 101 MHz, d_6-acetone: δ 160.9, 159.3, 140.7, 131.0, 129.5, 128.6, 127.1, 115.5, 106.0, 101.3, 70.1, 50.6, 44.4.

Determination of the Epoxy Equivalent Weight (EEW): The EEW of the RvOGly was evaluated by NMR titration using benzophenone as standard in deuterated chloroform (experimental details are given in ESI Section A).

"TPE-TAF/BDGE" vitrimer: Typically, 1 g (2.0 mmol, 5.9 meq COOH, HEW = 170 g/eq) of RvOH-TAF was quickly mixed manually directly in a PTFE mold with 1.07 g (5.9 meq epoxy, EEW = 185 g/eq) of RvOGly at room temperature (ca. 20 °C) until a light brown viscous homogeneous mixture was obtained. The mixture was left at least 3 h at room temperature for gelation. The resulting material (TPE-TAF/BDGE) was then removed from the molds and cured 10 h at 150 °C.

Instrumentation

NMR: ^{1}H, ^{13}C and ^{19}F were acquired on a Bruker Avance 400 MHz spectrometer at 23 °C. External reference was tetramethylsilane (TMS) with chemical shifts given in ppm. Samples were diluted in 0.5 mL of $CDCl_3$, DMSO-d_6 or acetone-d_6 depending on their solubility.

Mechanical characterizations: temperature ramps in elongation mode were carried out on Netzsch DMA 242 E Artemis cooled by liquid nitrogen. Uniaxial stretching of samples (1 × 3.5 × 12 mm^3) was applied while heating at a rate of 3 °C min^{-1} from −50 °C to 270 °C, keeping the frequency at 1 Hz. Curing monitoring experiments were performed on a ThermoScientific Haake Mars 60 rheometer equipped with a Peltier heating cell and a 8-mm plane-plane geometry. A 0.1 % deformation was applied to 8 mm diameter and 2 mm thickness circular samples at ω = 1 $rad.s^{-1}$ under a normal force of 100 grams every 2 minutes, and G' evolution over time was monitored. Stress relaxation experiments were performed with a 0.3 % torsional strain applied on 8 mm diameter and 2 mm thickness circular samples, and the rubbery modulus evolution with time was monitored.

TGA: thermogravimetric thermograms were recorded on a TA TGA G50 instrument using a 40 mL min^{-1} flux of nitrogen or synthetic air as purge gas. Approximately 10 mg of sample were used for each analysis. Ramps were applied at a rate of 20 °C min^{-1}.

DSC: analyses were carried out using a NETZSCH DSC200F3 calorimeter. The calibration was performed using adamantane, biphenyl, indium, tin, bismuth and zinc standards. Nitrogen was used as purge gas. Approximately 10 mg of sample were placed in perforated aluminum pans and the thermal properties were recorded at 20 °C min^{-1}. The reported values are the values measured during the second heating ramp.

Reprocessing: the material was grinded with a manual stainless steel coffee grinder (for DSC and DMA) or cut into 6 to 9 mm^3 pieces (for pictures) and then pressed in stainless steel molds for 2 h at 170 °C under 80 bars of pressure using a manual heating press.

Author Contributions

Conceptualization: FC, SC, ED, SL, EL, VL. Funding acquisition: SC, ED, EL, VL. Investigation: FC, SL. Methodology: all authors. Project administration: SC, ED, EL, VL. Supervision: FC, SC, ED, EL, VL. Validation: all authors. Visualization: FC. Writing – original draft: FC. Writing – review & editing: all authors.

Conflicts of interest

There are no conflicts to declare.

Acknowledgements

This work was funded by the Institut Carnot Chimie Balard CIRIMAT (16CARN000801).

Notes and references

1 W. Denissen, J. M. Winne and F. E. Du Prez, *Chem. Sci.*, 2016, **7**, 30–38.

2 N. J. Van Zee and R. Nicolaÿ, *Prog. Polym. Sci.*, 2020, **104**, 101233.

3 J.-P. Pascault, H. Sautereau, J. Verdu and R. J. J. J. Williams, *Thermosetting Polymers*, Marcel Dekker, Inc., New York, 2002.
4 M. Capelot, D. Montarnal, F. Tournilhac and L. Leibler, *J. Am. Chem. Soc.*, 2012, **134**, 7664–7667.
5 L. Leibler, M. Rubinstein and R. H. Colby, *Macromolecules*, 2002, **24**, 4701–4707.
6 C. J. Kloxin, T. F. Scott, B. J. Adzima and C. N. Bowman, *Macromolecules*, 2010, **43**, 2643–2653.
7 C. J. Kloxin and C. N. Bowman, *Chem. Soc. Rev.*, 2013, **42**, 7161–7173.
8 D. Montarnal, M. Capelot, F. Tournilhac and L. Leibler, *Science*, 2011, **334**, 965–968.
9 R. Hsissou, R. Seghiri, Z. Benzekri, M. Hilali, M. Rafik and A. Elharfi, *Compos. Struct.*, 2021, **262**, 113640.
10 J. Zheng, Z. M. Png, S. H. Ng, G. X. Tham, E. Ye, S. S. Goh, X. J. Loh and Z. Li, *Mater. Today*, 2021, **51**, 586–625.
11 Y. Yang, R. Boom, B. Irion, D. J. van Heerden, P. Kuiper and H. de Wit, *Chem. Eng. Process. Process Intensif.*, 2012, **51**, 53–68.
12 A. E. Krauklis, C. W. Karl, A. I. Gagani and J. K. Jørgensen, *J. Compos. Sci.*, 2021, **5**, 28.
13 D. A. Kissounko, P. Taynton and C. Kaffer, *Reinf. Plast.*, 2018, **62**, 162–166.
14 Y. Yang, Y. Xu, Y. Ji and Y. Wei, *Prog. Mater. Sci.*, 2021, **120**, 100710.
15 W. Alabiso and S. Schlögl, *Polymers*, 2020, **12**, 1660.
16 Y. Yang and M. W. Urban, *Chem. Soc. Rev.*, 2013, **42**, 7446–7467.
17 A. Adjaoud, L. Puchot and P. Verge, *ACS Sustain. Chem. Eng.*, 2022, **10**, 594–602.
18 T. Liu, C. Hao, S. Zhang, X. Yang, L. Wang, J. Han, Y. Li, J. Xin and J. Zhang, *Macromolecules*, 2018, **51**, 5577–5585.
19 B. P. Chang, A. K. Mohanty and M. Misra, *RSC Adv.*, 2020, **10**, 17955–17999.
20 M. Giebler, C. Sperling, S. Kaiser, I. Duretek and S. Schlögl, *Polymers*, 2020, **12**, 1148.
21 K. Tangthana-Umrung, Q. A. Poutrel and M. Gresil, *Macromolecules*, 2021, **54**, 8393–8406.
22 M. Capelot, M. M. Unterlass, F. Tournilhac and L. Leibler, *ACS Macro Lett.*, 2012, **1**, 789–792.
23 J. Wang, S. Chen, T. Lin, J. Ke, T. Chen, X. Wu and C. Lin, *RSC Adv.*, 2020, **10**, 39271–39276.
24 J. J. Lessard, L. F. Garcia, C. P. Easterling, M. B. Sims, K. C. Bentz, S. Arencibia, D. A. Savin and B. S. Sumerlin, *Macromolecules*, 2019, **52**, 2105–2111.
25 C. He, S. Shi, D. Wang, B. A. Helms and T. P. Russell, *J. Am. Chem. Soc.*, 2019, **141**, 13753–13757.
26 G. M. Scheutz, J. J. Lessard, M. B. Sims and B. S. Sumerlin, *J. Am. Chem. Soc.*, 2019, **141**, 16181–16196.
27 F. Gamardella, S. De la Flor, X. Ramis and A. Serra, *React. Funct. Polym.*, 2020, **151**, 104574.
28 L. Zhou, G. Zhang, Y. Feng, H. Zhang, J. Li and X. Shi, *J. Mater. Sci.*, 2018, **53**, 7030–7047.
29 A. Ruiz de Luzuriaga, N. Markaide, A. M. Salaberria, I. Azcune, A. Rekondo and H. J. Grande, *Polymers*, 2022, **14**, 3180.
30 H. Zheng, Q. Liu, X. Lei, Y. Chen, B. Zhang and Q. Zhang, *J. Polym. Sci. Part A Polym. Chem.*, 2018, **56**, 2531–2538.
31 H. Liu, H. Zhang, H. Wang, X. Huang, G. Huang and J. Wu, *Chem. Eng. J.*, 2019, **368**, 61–70.
32 X. Zhang, Y. Eichen, Z. Miao, S. Zhang, Q. Cai, W. Liu, J. Zhao and Z. Wu, *Chem. Eng. J.*, 2022, **440**, 135806.
33 X. Lei, Y. Jin, H. Sun and W. Zhang, *J. Mater. Chem. A*, 2017, **5**, 21140–21145.
34 Y. Nishimura, J. Chung, H. Muradyan and Z. Guan, *J. Am. Chem. Soc.*, 2017, **139**, 14881–14884.
35 S. Gao, Y. Liu, S. Feng and Z. Lu, *J. Mater. Chem. A*, 2019, **7**, 17498–17504.
36 J. Han, T. Liu, C. Hao, S. Zhang, B. Guo and J. Zhang, *Macromolecules*, 2018, **51**, 6789–6799.
37 T. Liu, S. Zhang, C. Hao, C. Verdi, W. Liu, H. Liu and J. Zhang, *Macromol. Rapid Commun.*, 2019, **40**, 1800889.
38 F. I. Altuna, V. Pettarin and R. J. J. Williams, *Green Chem.*, 2013, **15**, 3360–3366.
39 F. I. Altuna, C. E. Hoppe and R. J. J. Williams, *Eur. Polym. J.*, 2019, **113**, 297–304.
40 F. Cuminet, S. Caillol, É. Dantras, É. Leclerc and V. Ladmiral, *Macromolecules*, 2021, **54**, 3927–3961.
41 S. Lemouzy, F. Cuminet, D. Berne, S. Caillol, V. Ladmiral, R. Poli and E. Leclerc, *Chem. - A Eur. J.*, 2022, **28**, e202201135.
42 D. Berne, F. Cuminet, S. Lemouzy, C. Joly-Duhamel, R. Poli, S. Caillol, E. Leclerc and V. Ladmiral, *Macromolecules*, 2022, **55**, 1669–1679.
43 F. Cuminet, D. Berne, S. Lemouzy, E. Dantras, C. Joly-Duhamel, S. Caillol, E. Leclerc and V. Ladmiral, *Polym. Chem.*, 2022, **8**, 5255–5446.
44 R. P. Babu, K. O'Connor and R. Seeram, *Prog. Biomater.*, 2013, **2**, 8.
45 H. Nakajima, P. Dijkstra and K. Loos, *Polymers*, 2017, **9**, 523.
46 S. Caillol, *Natural Polymers and Biopolymers II*, MDPI, Basel, 2021.
47 M. A. Lucherelli, A. Duval and L. Avérous, *Prog. Polym. Sci.*, 2022, **127**, 101515.
48 S. Engelen, A. A. Wróblewska, K. De Bruycker, R. Aksakal, V. Ladmiral, S. Caillol and F. E. Du Prez, *Polym. Chem.*, 2022, **13**, 2665–2673.
49 A. Genua, S. Montes, I. Azcune, A. Rekondo, S. Malburet, B. Daydé-Cazals and A. Graillot, *Polymers*, 2020, **12**, 1–14.
50 Y. Y. Liu, J. He, Y. D. Li, X. L. Zhao and J. B. Zeng, *Compos. Commun.*, 2020, **22**, 100445.
51 C. Ocando, Y. Ecochard, M. Decostanzi, S. Caillol and L. Avérous, *Eur. Polym. J.*, 2020, **135**, 109860.
52 T. Liu, C. Hao, L. Wang, Y. Li, W. Liu, J. Xin and J. Zhang, *Macromolecules*, 2017, **50**, 8588–8597.
53 F. Chen, F. Gao, J. Zhong, L. Shen and Y. Lin, *Mater. Chem. Front.*, 2020, **4**, 2723–2730.
54 T. Vidil and A. Llevot, *Macromol. Chem. Phys.*, 2022, **223**, 2100494.
55 T. Liu, C. Hao, S. Zhang, X. Yang, L. Wang, J. Han, Y. Li, J. Xin and J. Zhang, *Macromolecules*, 2018, **51**, 5577–5585.
56 Y. Tao, L. Fang, M. Dai, C. Wang, J. Sun and Q. Fang, *Polym. Chem.*, 2020, **11**, 4500–4506.
57 A. Moreno, M. Morsali and M. H. Sipponen, *ACS Appl. Mater. Interfaces*, 2021, **13**, 57952–57961.
58 A. Adjaoud, L. Puchot and P. Verge, *ACS Sustain. Chem. Eng.*, 2022, **10**, 594–602.
59 M. Jasiński, L. Jasińska and M. Ogrodowczyk, *Cent. Eur. J. Urol.*, 2013, **66**, 144.
60 J. M. Sales and A. V. A. Resurreccion, *Crit. Rev. Food Sci. Nutr.*, 2014, **54**, 734–770.
61 W. Peng, R. Qin, X. Li and H. Zhou, *J. Ethnopharmacol.*, 2013, **148**, 729–745.
62 G. Chatel, R. Duwald, C. Piot and M. Draye, *Sci. Eaux Territ.*, 2019, **27**, 102.
63 H. Fretz, *Tetrahedron*, 1998, **54**, 4849–4858.
64 C. Chatalova-Sazepin, M. Binayeva, M. Epifanov, W. Zhang, P. Foth, C. Amador, M. Jagdeo, B. R. Boswell and G. M. Sammis, *Org. Lett.*, 2016, **18**, 4570–4573.
65 C. Aouf, C. Le Guernevé, S. Caillol and H. Fulcrand, *Tetrahedron*, 2013, **69**, 1345–1353.
66 Y. Tian, Q. Wang, L. Shen, Z. Cui, L. Kou, J. Cheng and J. Zhang, *Chem. Eng. J.*, 2020, **383**, 123124.
67 M. D. Garrison, M. A. Savolainen, A. P. Chafin, J. E. Baca, A. M. Bons and B. G. Harvey, *ACS Sustain. Chem. Eng.*, 2020, **8**, 14137–14149.

68 Y. Tian, M. Ke, X. Wang, G. Wu, J. Zhang and J. Cheng, *Eur. Polym. J.*, 2021, **147**, 110282.
69 H. Liu, H. Zhang, H. Wang, X. Huang, G. Huang and J. Wu, *Chem. Eng. J.*, 2019, **368**, 61–70.
70 M. Giebler, C. Sperling, S. Kaiser, I. Duretek and S. Schlögl, *Polymers*, 2020, **12**, 1148.
71 F. Gamardella, F. Guerrero, S. De la Flor, X. Ramis and A. Serra, *Eur. Polym. J.*, 2020, **122**, 109361.
72 Y. Nishimura, J. Chung, H. Muradyan and Z. Guan, *J. Am. Chem. Soc.*, 2017, **139**, 14881–14884.